

3-Dimensional numerical analysis of the Taylor vortex flow with a small aspect ratio (Dynamical condition for the determination of the final mode)

Yorinobu TOYA^{*1}, Takashi WATANABE^{*2}, Hiroyuki Furukawa^{*3}, Ikuo NAKAMURA^{*3}

^{*1} Nagano National College of Technology, 716 Tokuma Nagano 381-8550 Japan

^{*2} Nagoya University, Nagoya 464-8603 Japan

^{*3} Meijo University, Nagoya, 464-8502 Japan

e-mail: toya@me.nagano-nct.ac.jp

1. Introduction

One of the representative models with non-uniqueness in the nonlinear dynamical system is evidently the Taylor vortex flow between concentric cylinders with a rotating inner cylinder and a stationary outer cylinder. The flow field of the mode having the non-uniqueness is not necessarily confirmed as a unique mode but has multiple solutions against a condition. The Taylor vortex flow with a small aspect ratio which has multiple modes depending on the dynamical parameter expressed as a Reynolds Number and on the geometric parameter as an aspect ratio is reported^{(1),(2)}. Furthermore the experimental study that the ratio of the increment of the Reynolds Number and the final value of it resulting in for determining a final stable mode is reported⁽³⁾. However no numerical analysis of the influence for determination of the final mode is assumed to be reported in our knowledge.

The numerical analyses for the stability of the Taylor flow are reported as follows. The numerical studies for the Taylor vortex flow with the infinite annulus are reported by Cliffe^{(4),(5)}. They found the normal two-cell mode and the anomalous modes, and they compared the numerical results from the experimental results. And they also clarified the ten-cell mode. Watanabe, Furukawa and Nakamura⁽⁶⁾ reported the development of the cell mode in 2-dimensional numerical analysis for the nonlinear development of flow pattern. And the 3-dimensional numerical analysis is reported by Liao and Young⁽⁷⁾. However there are not enough studies to indicate the bifurcation problems between the modes.

This 3-dimensional numerical study clarifies a type of the dynamical condition, the ratio of the Reynolds number increment and the final value of the Reynolds Number, for the mode formation. The numerical conditions provided were the same with our previous experiment⁽³⁾. The numerical analysis adopted six kinds of acceleration ratio and the six kinds of final value of the increasing Reynolds number. And we found a few final modes, normal 4-cell mode, normal 2-cell mode and anomalous 4-cell mode. The numerical results can be compared with the experimental results. Furthermore developments of two kinds of spatially averaged energy and enstrophy of each mode are presented. This numerical study would indicate the dynamical condition for the bifurcation of the modes.

2. Basic equations

The dynamical and the geometric parameters in this numerical analysis are basically the same with them in the experiments in ref (3). Aspect ratio Γ between the height of the working fluid L and the clearance of the annulus $D = r_o - r_i$, where r_o is the radius of the outer cylinder and r_i is the radius of the inner cylinder. In this study Γ was constant and 4.0. Reynolds number, Re is defined by $\omega r_i D / \nu$, where ω is the angular velocity of the inner cylinder, D is the clearance of the annulus and ν is the kinematic viscosity of the fluid. Radius ratio between cylinders is 0.667. The upper and bottom ends of the annulus are solid.

Governing equations in the cylindrical coordinate system (r, θ, z) show Navier-Stokes equation and continuity equation.

$$\frac{\partial \mathbf{u}}{\partial t} + \nabla \cdot (\mathbf{u} \mathbf{u}) = -\nabla p + \frac{1}{Re} \Delta \mathbf{u}$$

$$\nabla \cdot \mathbf{u} = 0$$

where $\mathbf{u} = (u, v, w)$. And the convective term in the equation of motion is denoted as a conservative form by adopting the calculation

method mentioned after. The equation of motion in the 3-dimensional cylindrical coordinate system is shown as follows.

$$\begin{aligned}
& \frac{\partial u}{\partial t} + u \frac{\partial u}{\partial r} + \frac{v}{r} \frac{\partial u}{\partial \theta} + \omega \frac{\partial u}{\partial z} - \frac{v^2}{r} \\
& = -\frac{\partial p}{\partial r} + \frac{1}{\text{Re}} \left(\frac{\partial^2 u}{\partial r^2} + \frac{1}{r} \frac{\partial u}{\partial r} - \frac{u}{r^2} + \frac{1}{r^2} \frac{\partial^2 u}{\partial \theta^2} - \frac{2}{r^2} \frac{\partial v}{\partial \theta} + \frac{\partial^2 u}{\partial z^2} \right) \\
& \frac{\partial v}{\partial t} + u \frac{\partial v}{\partial r} + \frac{v}{r} \frac{\partial v}{\partial \theta} + \omega \frac{\partial v}{\partial z} + \frac{uv}{r} \\
& = -\frac{1}{r} \frac{\partial p}{\partial \theta} + \frac{1}{\text{Re}} \left(\frac{\partial^2 v}{\partial r^2} + \frac{1}{r} \frac{\partial v}{\partial r} - \frac{v}{r^2} + \frac{1}{r^2} \frac{\partial^2 v}{\partial \theta^2} - \frac{2}{r^2} \frac{\partial u}{\partial \theta} + \frac{\partial^2 v}{\partial z^2} \right) \\
& \frac{\partial w}{\partial t} + u \frac{\partial w}{\partial r} + \frac{v}{r} \frac{\partial w}{\partial \theta} + w \frac{\partial w}{\partial z} \\
& = -\frac{1}{r} \frac{\partial p}{\partial z} + \frac{1}{\text{Re}} \left(\frac{\partial^2 w}{\partial r^2} + \frac{1}{r} \frac{\partial w}{\partial r} + \frac{1}{r^2} \frac{\partial^2 w}{\partial \theta^2} + \frac{\partial^2 w}{\partial z^2} \right)
\end{aligned}$$

A kind of stream functions Ψ_1 and Ψ_2 which are similar to the Stokes' stream function Ψ is adopted for flow visualization. Radius component u and axial component w are expressed as a function Ψ_1 and another function Ψ_2 respectively as follows.

$$u = -\frac{1}{r} \frac{\partial \Psi_1}{\partial z} \quad w = \frac{1}{r} \frac{\partial \Psi_2}{\partial r}$$

In order to visualize the flow field, the stream function Ψ which was averaged by Ψ_1 and Ψ_2 with some kinds of weights was used.

Boundary conditions of the velocity components on the cylinder walls and both end walls were non-slip conditions. Initial velocity was zero over the whole flow field.

In order to investigate the temporal development of the Taylor vortex flow, a spatially averaged energy (E) and a spatially averaged enstrophy (Ω) are defined as follows.

$$E = \frac{1}{V} \int_V \frac{\mathbf{u}^2}{2} dV \quad \Omega = \frac{1}{V} \int_V \frac{\boldsymbol{\omega}^2}{2} dV$$

where a vorticity $\boldsymbol{\omega} = (\omega_r, \omega_\theta, \omega_z)$.

3. Numerical methods

The MAC method was used as a basic solution procedure. The time integration was the explicit method and the spatial differentiation was the QUICK method for the convection terms and the second-order central difference method for other terms. A hybrid method of SOR and ILUCGS was used to solve the Poisson equation.

The staggered grid was adopted. The numbers of the grid in a respective direction should be an important factor in forming a flow field. In our preliminary analysis, the optimum grid numbers was investigated. The number of grid points in the radial direction was 21, the number of azimuthal direction grid points was 20 and the number of axial direction grid points was 84.

The acceleration of the increment of Reynolds number is shown in Table 1. The Reynolds number was increased lineally up to the final value of the Reynolds number.

Table1 Acceleration of the Reynolds number

		Acceleration Dimensionless Time					
		1	2	3	4	5	6
Re	253	5.14	2.57	1.715	1.285	1.03	0.855
	488	19.13	9.565	6.375	4.785	3.77	3.19
	740	43.955	21.98	14.725	10.99	8.79	7.255
	993	79.335	39.61	26.395	19.79	15.835	13.21
	1228	121.085	60.545	40.375	30.27	24.215	20.17
	1487	176.83	88.415	58.96	44.21	35.375	29.455

The numerical condition provides the 6 kinds of final values of the Reynolds number and 6 kinds of acceleration ratio of the increment of the Reynolds number. These conditions adopted were the same as those in the experiment. The dimensionless time interval was taken at 0.005 and the dimensionless time step was up to 1000.

4. Results

4.1 Mode configuration

The vector lines of the time development of a primary normal four-cell mode, N4 at $Re=1228$ and $ac=2$ is shown in Fig.1. In each diagram the left side of the flow field is the inner cylinder and the right side is the outer cylinder. Other modes we found were a secondary normal two-cell mode, N2 and a secondary anomalous four-cell mode, A4. For differences between N4 and A4 the bottom cell in N4 rotates clockwise and the bottom cell in A4 rotates counter clockwise. And this formation process in the numerical analysis was similar to the results in experiment.

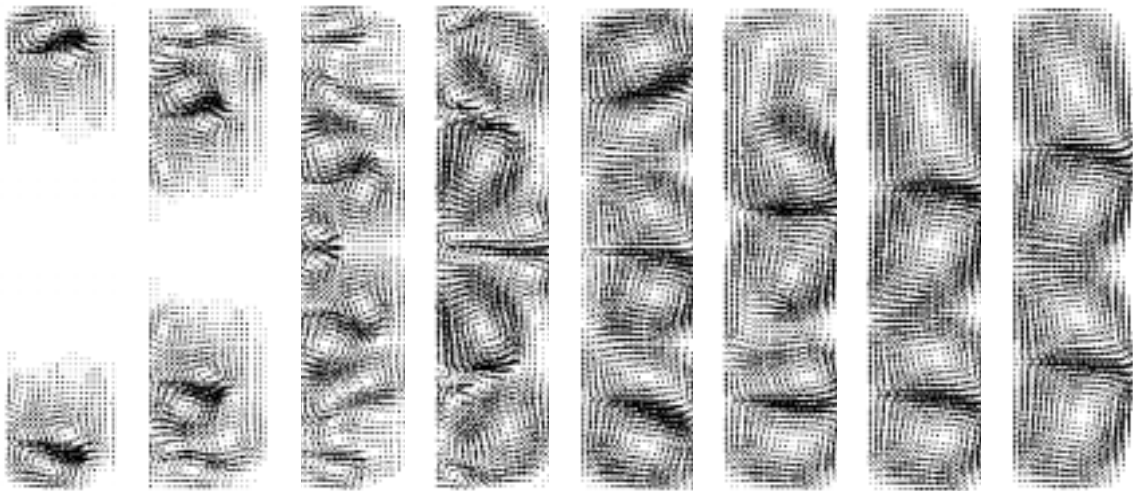


Fig.1 Development of the primary 4-cell mode $Re=1228$ $Ac=2$

The left side is the inner cylinder and the right side is the outer cylinder

4.2 Comparison for the final modes with experimental results

Comparison of the final modes formed by increasing Re with the experimental results is shown in the numerical results in Table 2 and the experimental one in Table 3. In each table, the column denotes Re and the row denotes the Ac . The experiment has been conducted a hundred times in each condition and the mode that most frequently emerged in each condition was decided as the final mode. The numerical results are in good agreement with the results in the experiment in many conditions.

Table 2 Final mode in Numerical result

		Acceleration					
		1	2	3	4	5	6
Re	253	N4	N4	N4	N4	N4	N4
	488	N2	N4	N4	N4	N4	N4
	740	N2	N4	N4	N4	N4	N4
	993	N4	N4	N4	N4	N4	N4
	1228	N2	N4	N4	N4	A4	A4
	1487	N2	N4	N4	N4	N4	N4

Table 3 Final mode in Experimental result

		Acceleration					
		1	2	3	4	5	6
Re	253	N4	N4	N4	N4	N4	N4
	488	N4	N4	N4	N4	N4	N4
	740	N4	N4	N4	N4	N4	N4
	993	N4	N4	N4	N4	N4	A4
	1228	N4	A4	A4	A4	A4	A4
	1487	N4	N4	N4	N4	N4	N4

4.3 Mean energy and mean entropy

The development of the spatially averaged energy and the spatially averaged entropy of the N4 and the A4 are shown in Figs. 2 and 3. Evidently both of the mean energy and the mean entropy of each mode are different.

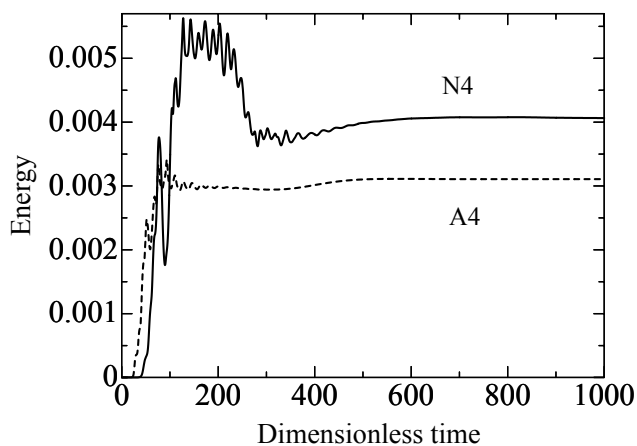


Fig. 2 Mean Energy $Re=1228$ $Ac=2$

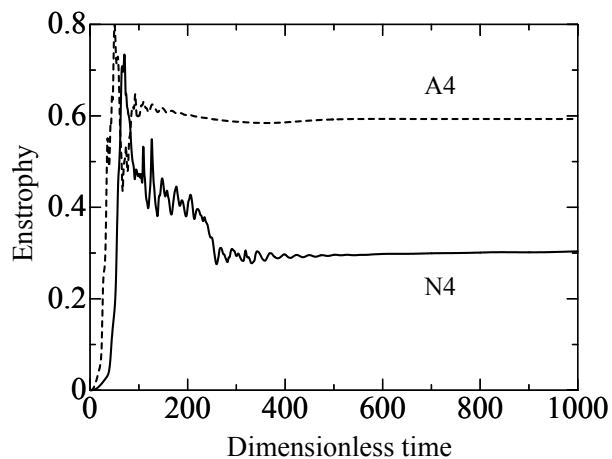


Fig.3 Mean Enstrophy $Re=1228$ $Ac=2$

5. Discussion

The Taylor vortex flow is a paradigm in nonlinear dynamical system. Especially the Taylor vortex flow has multiple modes in the same condition due to the non-uniqueness. We consider that the factor which influenced to the decision of the final mode is how the Re increased up to the final value. That is why we found the modes including the primary mode and the secondary modes could be formed by the difference of the way of the increasing Re in our experiment. However we could not confirm the definite condition, because the condition was clarified only by probability in the experiment. The 3-dimensional numerical analysis has possibility to shed light on the factor of the decision of the final mode. The formation processes of the modes were in good agreement with the experimental results. And the final modes were compared with the experimental results and the comparison was in good agreement with the experiment. The mean energy and the mean enstrophy in time development were shown and the differences of process and the final value between the modes were clarified.

6. Conclusion

Development process of the Taylor vortex flow with a small aspect ratio was analyzed numerically and the condition of the decision of the final mode was investigated. The condition, the final value of the Reynolds number and the ratio of the increment of the Reynolds number, determines the final mode. And the numerical results were in agreement with the experimental results. The development of the spatially averaged energy and the enstrophy of each mode were analyzed and both characteristics indicate the process of the mode formation.

References

- [1] K. A. Cliffe, T. Mullin, *A numerical and experimental study of anomalous modes in the Taylor experiment*, J. Fluid Mech., 153, 243-258, 1985.
- [2] I. Nakamura, Y. Toya, *Existence of extra vortex and twin vortex of anomalous mode in Taylor vortex flow with a small aspect ratio*, Acta Mechanica 117, 33-46, 1996.
- [3] I. Nakamura, Y. Toya, *Configurational Condition of Mode of Multiple Taylor Vortex Flow: In the case of a symmetric condition*, Trans. Japan Soc. Mech. Engineers, vol.60 No.571, 723-729, 1994, (in Japanese).
- [4] K. A. Cliffe, *Numerical calculation of two-cell and single-cell Taylor flows*, J. Fluid Mech., 135, 219-233, 1983.
- [5] K. A. Cliffe, *Numerical calculation of the primary flow exchange process in the Taylor problem*, J. Fluid Mech., 197, 57-79, 1988.
- [6] T. Watanabe, H. Furukawa and I. Nakamura, *Nonlinear development of flow patterns in an annulus with decelerating inner cylinder*, Physics of Fluids, Vo.14, No.1, 333-341, 2002.
- [7] C. B. Liao, D. L. Young, *Numerical simulation of three-dimensional Couette-Taylor flows*, Int. J. Numerical Methods in Fluids, 29, 827-847, 1999.